

## DOPPLER ULTRASOUND STUDIES OF VARIATION BETWEEN MEAN FLOW VELOCITY AND DOPPLER ANGLE IN THE COMMON CAROTID ARTERY WALL-LESS PHANTOM

Pam S.D<sup>\*1</sup>, Sirisena A.U.I<sup>\*2</sup>, Dakok K.K<sup>\*3</sup>, Nabasu S.E<sup>\*4</sup>

<sup>\*1,2</sup>Jos University Teaching Hospital Jos, Plateau State, Nigeria.

<sup>\*3,4</sup>Department Of Physics, Plateau State University Bokkos, P.O Box 2012, Plateau Sate, Nigeria.

### ABSTRACT

**Objective:** Flow phantoms with anatomically realistic geometry and high acoustic compatibility with real vessels are reliable tools in vascular ultrasound studies. We present a common carotid artery (CCA) wall-less phantom for ultrasound studies of relationship between mean flow velocity and Doppler angle. **Methods:** The phantom was constructed with a lumen diameter of 6.0 mm within normal human carotid geometry. The tissue mimicking material (TMM) consists of konjac, carrageenan and gelatin as basic components mixed with other suitable components. The blood-mimicking fluids (BMF) were prepared by mixing propylene glycol and Glucose, while poly 4-methystyrene and cholesterol serve as scattering particles. The constructed phantom was scanned using ultrasound machine to measure the mean flow velocities through the lumen. **Results:** The BMF mean flow velocity in the CCC wall-less phantom increased with increase in the Doppler angle while the velocity errors decreased. Measurements of flow indices were best carried out at a flow rate of 1500 ml/min with entrance length of 3 cm (where the flows were laminar) and the Doppler angle set at 60° around the center of the flow. **Conclusion:** Therefore, teaching and learning of Doppler ultrasound of the CCA can be carried out using in-vitro method since a similar result is obtained as found in in-vivo method on variation between mean flow velocity and Doppler angle.

**Keywords:** Tissue Mimicking Material; Blood Mimicking Fluid; Common Carotid Artery; Mean Flow Velocity; Doppler Ultrasound; Wall-Less Phantom.

### I. INTRODUCTION

Doppler ultrasonography measures the speed of blood and flow rate by employing B-mode ultrasound imaging which uses pulse-echo transmission, detection, and display techniques (Mehra, 2010; Grand-perret et al., 2018). Rapidly moving targets, such as red cells in the bloodstream, produce echoes of low amplitude that are not usually displayed, resulting in a relatively anechoic pattern within the lumens of large vessels. When high-frequency sound bounces on a stationary interface, the reflected signal has essentially the same frequency or wavelength as the transmitted sound. But if the reflecting interface is moving with respect to the sound beam emitted from the transducer, there is a change in the frequency of the sound scattered by the moving object. This change in frequency is directly proportional to the velocity of the reflecting interface relative to the transducer due to what is known as the Doppler Effect.

The advent of Doppler ultrasound (DU) enables the detection and measurement of the speed of moving objects and fluids within a system. Imaging devices are able to calculate the coordinates from which echoes originate, and these together with knowledge of the echo amplitudes allow cross-sectional images of the body to be constructed. In medical ultrasound, the transducer sends a signal ( $f_0$ ) which is reflected by the moving body. The difference between this transmitted frequency and the reflected frequency ( $f_r$ ) gives the Doppler frequency,  $f_d$  (Holen, 1985; Oqlat, et al., 2018). This Doppler shift frequency is influenced by the angle ( $\theta$ ) between the direction of flow and the axis of the ultrasound beam toward the transducer. Mathematically, it can be expressed in equation 1 (Holen, 1985) as;

$$f_d = f_r - f_0 = \frac{2f_0v}{c} \cos \theta \dots\dots\dots 1$$

Where  $c$  represents the speed of sound and  $v$  is the flow velocity. DU has been a means by which levels of stenosis are examined using blood flow measurements through the vessel of interest (Hoskins, 2008; Evans et al., 2011; Mohler et al., 2012; Mohammadkarim et al., 2018). This is possible due to new improvements in science and technology which measures the velocity of moving fluids (Evans et al., 2011; Busch et al., 2016;

Castro et al., 2017). In most clinical applications, the direction of the ultrasound beam is usually directed toward or away from the direction of flow, and the ultrasound beam usually approaches the moving target at an angle known as the Doppler angle (angle between the direction of blood flow and the ultrasound beam) as shown in figure 1. The maximum Doppler shift occurs when the sound waves are parallel to the direction of flow but the ideal value for most examinations is between 30° to 60° (Arash et al., 2017).

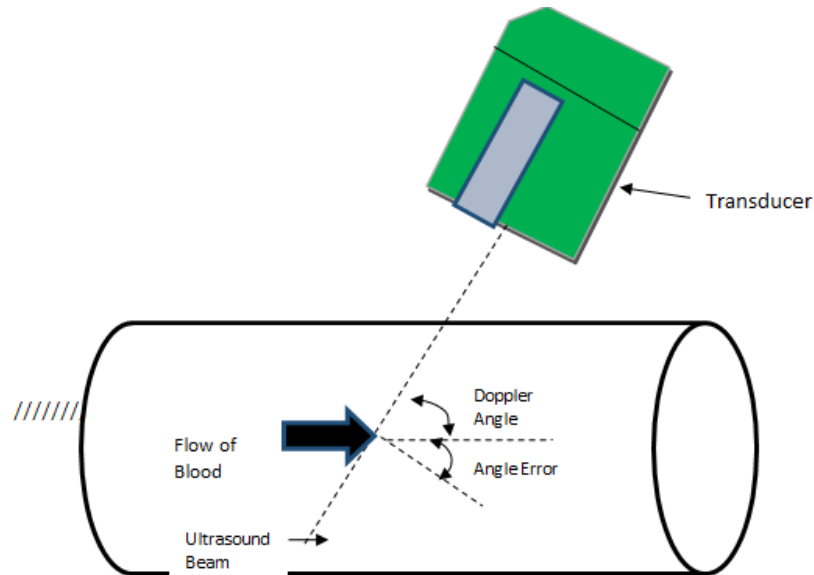


**Figure 1:** Angle between the ultrasound beam and the direction of blood flow.

The aim of this research is to investigate variation between flow velocity in the common carotid artery (CCA) and Doppler angle by in-vitro method with the aid of a DU machine. Results gotten from this research will help in teaching and learning of DU techniques without necessarily using human beings as subjects. Most teaching and learning process on DU techniques particularly in developing countries are carried out using humans as part of the needed tools. This is a difficult task as not many people are willing to offer themselves to be used for such teaching and learning. Another challenge associated with using humans for teaching, learning and research is the difficulty to be able to get ethical clearance and on time. This necessitates the need to explore in-vitro means of carrying out teaching, learning and research that will give results close to what is obtainable using in-vivo methods.

## II. MATERIALS AND METHODS

### 2.1 Materials:

The material required for this research are made up of chemical items and apparatus needed to prepare blood mimicking fluids and CCA wall-less phantom. Chemicals used for preparing BMF include propylene glycol (PG), polyethylene glycol (PEG Mw 200), D(+)-Glucose (DG), total cholesterol, Poly (4-methylstyrene) and Benzalkonium Chloride (BKC) all purchased from Sigma Aldrich company. Items needed to prepare a tissue mimicking material (TMM) for the CCA wall-less phantom fabrication include; Silicon Carbide Powder, Aluminum Oxide, gelatin, conjac root glucomannan powder, carrageenan powder, Potassium Chloride and glycerol also gotten from Sigma Aldrich.

### 2.2 Methods

**a. Blood Mimicking Fluids preparation:** 90 % weight/weight (w/w) of distilled water was measured using a measuring cylinder and 5% w/w composition of PG was weight as well as 5% w/w of glucose in a fume cupboard using a chemical balance. The distilled water was first poured into the beaker, followed by the glucose with thorough stirring to ensure that the glucose dissolves completely. Finally, the PG was added and the whole component placed on a magnetic stirrer hot plate.

The stirring plate was set to operate at 700 revolutions per minute (rpm) for 20 minutes at a temperature of 37°C after which the vacuum pump is used to degas the fluid for about 30 minutes. The procedures above were repeated four more times but with different percentages of distilled water and glucose while the amount of PG

remained fixed at 5% w/w composition. The five (5) samples together with 100% distilled water were then tested for their densities, viscosities, speed of sound, attenuation and backscatter properties. A correlation and regression analysis of the results using the statistical package for social sciences (SPSS) software between the density and the amount of glucose in the fluids resulting to the regression equation 3.1 ( $R^2 = 0.9996$ ):

$$\text{Density } (\rho) = 0.00426(\text{amount of DG}) + 0.993 \dots \dots \dots 2$$

With equation 2, which was useful in determining the exact amount of DG required to produce a specific density, 11% w/w of glucose was required to mix with 5% w/w of PG and 84% w/w of distilled water to produce exactly a mixture fluid with a density of 1.040 g/cm<sup>3</sup>, a value required to match with the density of poly (4-methylstyrene) scatter. This allows the scatter particles to remain neutrally buoyant in the fluid mixture. Finally, the BMF was produced by mixing the required amount of scatter particles, poly 4-methylstyrene (0.8% w/w) with the mixture fluid (5% w/w of PG, 11% w/w of DG and 84% w/w of water). The BMF was then placed on the stirrer plate and two drops of 50% anti-fungal agent (Benzalkonium Chloride) was added, it was then stirred for about 30 minutes and degassed for about an hour to remove the air bubbles. The above procedures were followed to prepare another BMF but replacing poly 4-methylstyrene with total cholesterol as scatter particles as described by Dakok et al., 2021.

**b. Fabrication of a CCA wall-less Phantom**

The CCA wall-less phantom was fabricated through a number of processes. First, the phantom box was designed and constructed, followed by preparing the TMM, finally by casting the TMM inside the phantom box. The TMM adopted for the wall-less phantom in this research is the Konjac-Carrageenan (KC) and gelatin based mimicking material (Ammar et al., 2018a) because it has the advantage of not being ruptured during high flow unlike the KC-based wall-less phantoms that suffers from rupturing. Table 1 summarises the components of the items used in preparing the TMM with their percentage combination. The detailed procedure for achieving this fabrication is summarised in figure 2.

**Table 1:** Constituents of Konjac-Carrageenan (KC) and gelatin (from bovine skin) tissue mimicking material (TMM) for wall-less phantom

Name of substance	Percentage Composition (%)	Function
Distilled water	84.0	Serves as water component of the tissue
Silicon Carbide	0.53	Serves as scatters
Al <sub>2</sub> O <sub>3</sub> powder (3 μm)	0.96	Serves as scatters
Al <sub>2</sub> O <sub>3</sub> powder (0.3 μm)	0.89	Serves as Scatters
Konjac powder	1.5	For gel formation
Carrageenan powder	1.5	For gel formation
Potassium Chloride	0.7	To fertilize the TMM
Glycerol	9.0	To mimic the acoustic properties of the tissue
Gelatin	0.92	To make the TMM strong
50% Benzalkonium Chloride		Preservative

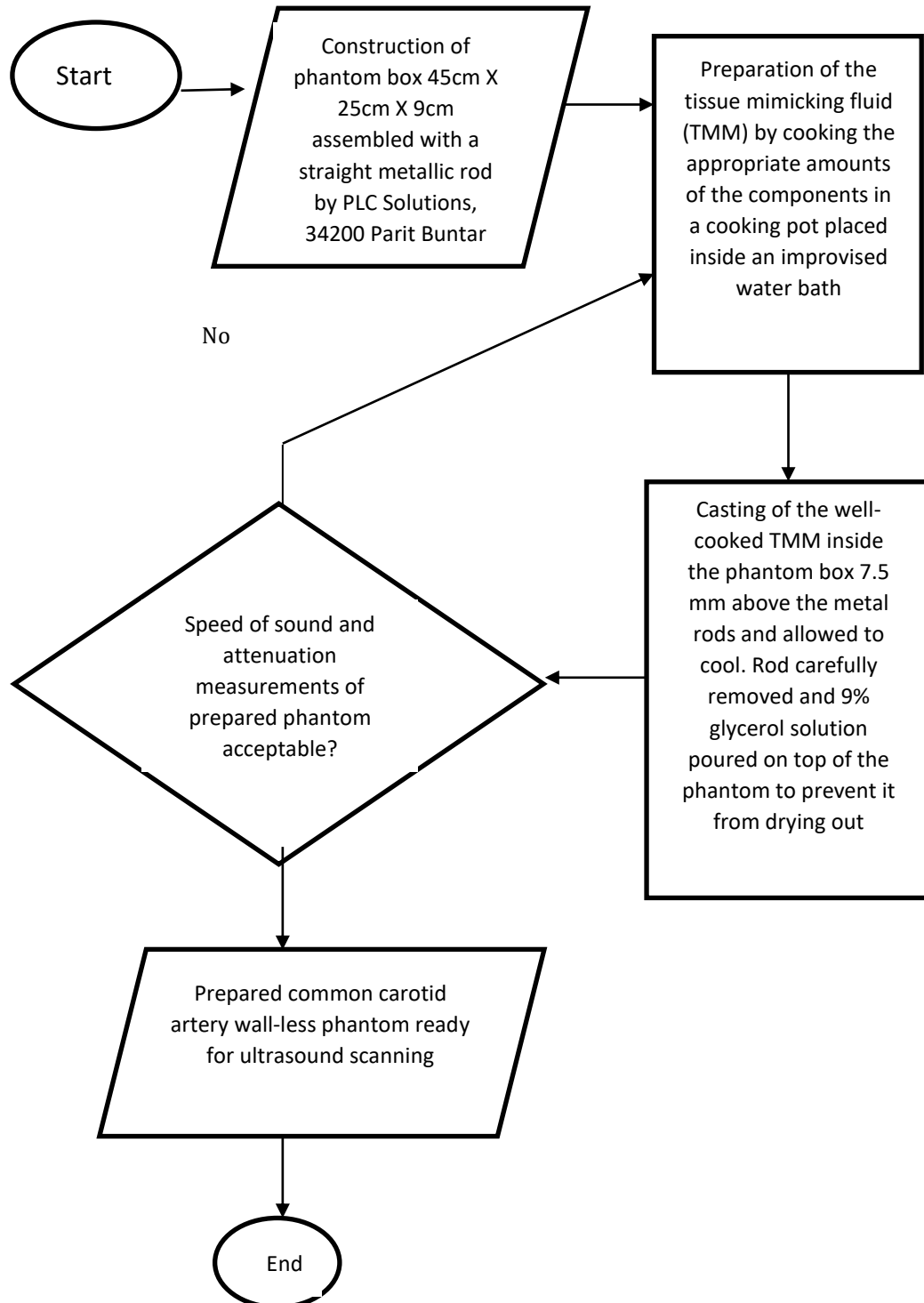


**Figure 2:** Flowchart Summarizing the Procedure for Preparation and Casting of Tissue Mimicking Material

**c. Measurements of Physical and Acoustic Properties:** The densities of the BMF fluids samples (figure 3a) were measured using a portable Density Meter (DMA 35). The strip attached to the meter was pressed down and dipped in the fluid. It was released to draw up the fluid inside the strip by suction pressure, while the density reading was recorded automatically by the meter in just few seconds with an accuracy of 0.01 g/cm<sup>3</sup>. About 700 cm<sup>3</sup> of each BMF fluid was required for the viscosity measurements. The spindle L1 was selected for viscous liquid, it was attached to the electronic rotational viscometer (ERV), and then lowered into the fluid (figure 34b) while the ERV was switched on. The spindle rotates inside the liquid for few minutes until a steady

value of the viscosity was recorded due to the viscous resistance from the fluid (Kim et al., 2015; Kin et al., 2019; Chunhwa et al., 2020). The speed of sound was measured by pulse echo (PE) method using the A-scan Gampt machine. The arrangement for this measurement is shown in (figure 3c) where the time of flight (TOF) between the highest two peaks of the transmitted and reflected waves was measured (Ammar et al., 2018b). The values for the speed of sound for the liquids were calculated using equation 3

$$\text{speed of sound (c)} = \frac{2d}{t} \dots\dots\dots 3$$

Where d is the thickness or depth of the sample and t is the time of flight of the signal wave pulse from the reflected wave.

To measure the attenuation of the samples, the amplitude voltages of the highest two similar peaks for transmitted and received signals were respectively measured. These values were substituted in equation 4 and the attenuation values were calculated.

$$\alpha = \frac{1}{x_1 - x_2} \ln \frac{A_2}{A_1} \dots\dots\dots 4$$

Where  $x_1$  and  $x_2$  is the difference in distance (depth) of sample in millimetre,  $A_1$  is the amplitude of transmitted signal wave,  $A_2$  is the amplitude of received signal wave.

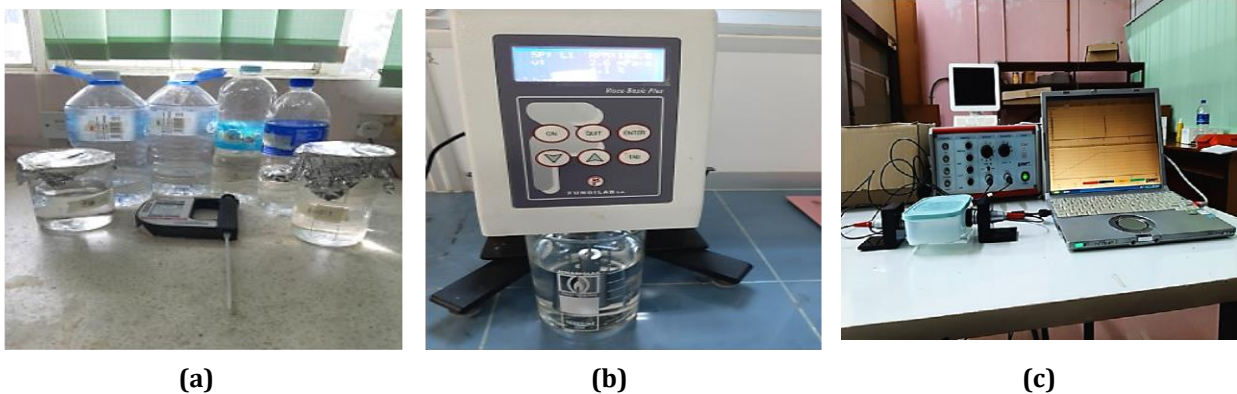


**Figure 3:** (a) Density meter (DMA 35) to measure the density of the aqueous solutions, (b) Rotational Viscosity Meter measuring the viscosity of the mixture fluids, (c) Measurement of the acoustic properties of solutions using the A-scan Gampt technique

The backscatter power of the BMF was measured at different radio frequency signals by calculating the average power spectrum through applying the Fast Fourier Transform (FFT) generated by the A-scan Gampt software at 5 MHz. The backscatter coefficients were directly read on the screen of the A-mode PE technique during the ultrasound scan. A digital clinical Hitachi ultrasound scanning machine connected with a linear array transducer (EUP-L74M) with frequencies ranging from 5 to 13 MHz was used to get image information from vascular wall-less flow phantom. Measurements of the mean flow velocities for both BMF samples were carried out by colour Doppler and Pulse-wave (PW) Doppler systems and results were recorded. The angle of beam (Doppler angle) was adjusted and focused at the centre of the flow and ensuring that the beam and the flow met at different angles from 0° to 80° with the required sample volume and entrance length 3 cm.

### III. RESULTS AND DISCUSSION

It is already known that velocity of blood flow in the carotid artery phantoms are mostly measured with the Doppler angle set within a range of 30° to 60° (Kenwright et al., 2015; Oglat et al., 2018b). More accurate measurements using the Doppler ultrasound machine are usually carried out when the angle is positioned at 60°. In this research, we performed the Doppler ultrasound measurements of mean velocity flow for the two BMF samples through the 6.0 mm diameter wall-less phantom at different angles from 0° to 80° with one of the results displayed as figure 5.

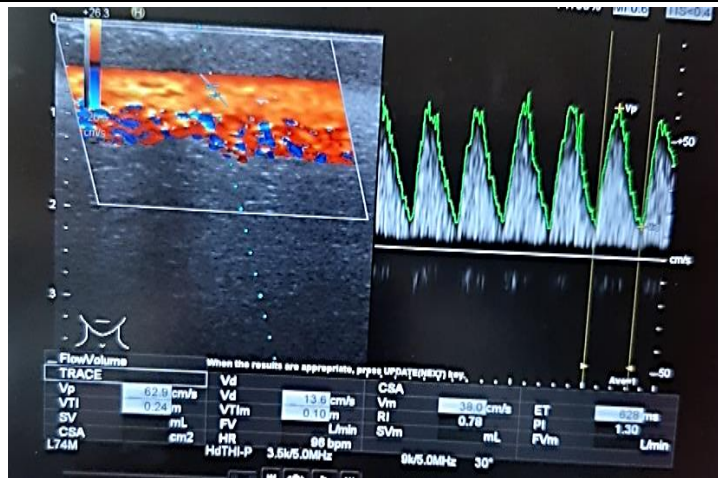


**Figure 4:** Flow velocity indices for BMF with glucose in 6.0 mm phantom at 30° Doppler angle

Percentage absolute mean velocity percentage difference were calculated using the formula in equation 5 (Steinman et al., 2001):

$$\% \text{ absolute mean velocity difference} = \frac{v_1 - v_2}{v_1} \times 100 \dots\dots\dots 5$$

Where  $v_1$  is the real velocity gotten from the relationship between flow rate and mean velocity in a vessel (mean velocity = flow rate/vessel area), and  $v_2$  is the mean velocity measured by the ultrasound machine for a flow rate of 1500 ml/min. The results for the percentage absolute mean velocity difference are shown in table 2.

**Table 2:** Variation between mean velocity of BMF samples with Doppler angle for 6.0 mm wall-less phantom.

Doppler Angle (degrees)	BMF with Glucose		BMF with cholesterol	
	$v_1$ (cm/s) ±2.00	Absolute % error	$v_2$ (cm/s) ±2.00	Absolute %error
0	15.3	80.0	10.0	87.0
10	24.0	68.7	18.2	76.2
20	30.1	60.7	26.8	65.0
30	38.0	50.4	33.9	55.7
40	48.9	36.2	43.0	43.9
50	55.1	28.1	51.6	32.6
60	69.9	8.8	65.2	14.9
70	102.0	33.2	98.9	29.1
80	186.0	142.8	180.0	135.0

The BMF velocity increased with increase in the Doppler angle while the velocity errors decreased. This is because the velocity is inversely related to the cosine of the angles and the ultrasound beam becomes more aligned towards the direction of the flow as the angle is increased (Holen, 1985 ). The minimum velocity errors for both BMF samples occurred at 60° making this angle the best for ultrasound measurement of blood flow in the carotid artery phantom. Therefore, measurements of flow indices can be best carried out at a flow rate of 1500 ml/min with entrance length of 3 cm (where the flows were laminar) and the Doppler angle set at 60° around the center of the flow (Roman et al., 2006; Lee, 2013; Arash et al., 2017).

#### IV. CONCLUSION

This study has presented an in-vitro method of verifying the variation between mean flow velocity in the CCA wall-less phantom with Doppler angle. Results showed a correspondence with existing literature on the variation between flow velocity and the angle of insonation in the human CCA. It goes to show that instead of using human subjects for teaching and learning on Doppler ultrasonography technique, phantoms can be used

to achieved almost the same results. This has solved the problem associated with difficulty in getting human subjects and ethical clearance for carrying out researches.

### ACKNOWLEDGMENT

We acknowledge the contributions of all the authors providing technical support and editing of the manuscript. Dr. Pam S.D performed the experiment and contributed in drafting of the manuscript. Dr. Dakok K.K, Dr. Sirisena and Mr Nabasu Seth contributed with essential materials needed for the manuscript drafting and also participated in prove reading the manuscript. All authors read and approved the final manuscript.

#### Financial support and sponsorship

Not applicable

#### Conflicts of interest

Not applicable

### V. REFERENCE

- [1] Ammar, A. O., Matjafri, M., Suardi, N., Oqlat, M. A., Oqlat, A. A., Abdelrahman, M. A., Farhat, O. F., Ahmad, M. S., Alkhateb, B. N., Gemanam, S. J., Shalbi, S. M., Abdalrheem, R., Shipli, M., Marshdeh, M. (2018a). Characterization and Construction of a Robust and Elastic Wall-Less Flow Phantom for High Pressure Flow Rate Using Doppler Ultrasound Applications. *Natural and Engineering Sciences*, 3(3), p.359–377.
- [2] Ammar A. O., Matjafri M. Z., Nursakinah S., Mohammed. A. O., Mostafa A A., Ahmad A. O., Raed A. (2018b). Measuring The Acoustical Properties of Fluids and Solid Materials Via Dealing With A-SCAN ( GAMPT ) Ultrasonic Measuring The Acoustical Properties of Fluids and Solid Materials Via Dealing With A-SCAN (GAMPT) Ultrasonic.The International Conference of Solid State Science and Technology, p.1–7.
- [3] Arash A., Xiaozhou M., Somesh L., Mazumdar V., Bijal J. V. (2017). Tissue Harmonic Imaging and Doppler Ultrasound Imaging. *Abdominal Imaging* 2, p. 24–36.
- [4] Busch, K. J., Kiat, H., Stephen, M., Simons, M., Avolio, A., & Morgan, M. K. (2016). Cerebral hemodynamics and the role of transcranial Doppler applications in the assessment and management of cerebral arteriovenous malformations. In *Journal of Clinical Neuroscience*, 30, pp.24–30.
- [5] Castro, C. F., Sousa, L. C., Henriques, H. A. M., António, C. C., Santos, R., Castro, P., & Azevedo, E. (2017). Hemodynamic Abnormalities in a Carotid Bifurcation Based on Doppler Ultrasound Imaging. *02(05)*, p.85–95.
- [6] Chunhwa, I., Lee, D., Ahn, K. H., & Oh, J. S. (2020). Viscosity Measurement of Whole Blood with Parallel Plate Rheometers. *The Korean BioChip Society and Springer*, p.1–6.
- [7] Dakok K. K., Matjafri M. Z., Suardi N., Oqlat A. A., Nabasu S. E. (2021). A blood-mimicking fluid with cholesterol as scatter particles for wall-less carotid artery phantom applications. *J Ultrason*; 21: e219–e224. doi: 10.15557/JoU.2021.0035
- [8] Evans, D. H., Jensen, J. A., & Nielsen, M. B. (2011). Ultrasonic colour Doppler imaging. *Interface Focus*, 1(4), p.490–502.
- [9] Grand-perret, V., Jacquet, J., Leguérney, I., Benatsou, B., Grégoire, J., Willoquet, G., Bouakaz, A., Lassau, N., & Pitre-champagnat, S. (2018). A Novel Microflow Phantom Dedicated to Ultrasound Microvascular Measurements. *Ultrasound Imaging*, 40(5), p.325–338.
- [10] Holen, J. (1985). Introduction to Vascular Ultrasonography. *Radiology*, 154(2): p. 355–367
- [11] Hoskins, P. R. (2008). Simulation and Validation of Arterial Ultrasound Imaging and Blood Flow. *Ultrasound in Medicine and Biology*, 34(5), p.693–717.
- [12] Kenwright, D. A., Laverick, N., Anderson, T., Moran, C. M., & Hoskins, P. R. (2015). Wall-less flow phantom for high-frequency ultrasound applications. In *Ultrasound in Medicine and Biology*, 41(3), pp.890–897.
- [13] Kim You Ra, Ka Young Moon, Nam Chun Cho, E. Y. K., & Lee, D. W. (2015). Measuring Blood Viscosity in Normal Tension Glaucoma Patients. *J Korean Ophthalmol Soc*, 56(5), p.753–758.
- [14] Kin H.L., Winnie C.C., Alice P. S., Lai Y.Y., Ling C., Ming C.L., Rubee P. M., Wing H.T., Juliana C.N. (2019). Augmented Velocity Index\_ A New Doppler Index Associated with Arterial Stiffness - ScienceDirect.

- 
- Ultrasound in Medicine & Biology, 45(10), p.2747–2757.
- [15] Lee, W. (2013). General principles of carotid Doppler ultrasonography. *Ultrasonography*, 33(1), p.11–17.
- [16] Mehra, S. (2010). Role of duplex doppler sonography in arterial stenoses. *Journal, Indian Academy of Clinical Medicine*, 11(4), p.294–299.
- [17] Mohammadkarim, A., Mokhtari-Dizaji, M., Kazemian, A., & Saberi, H. (2018). Hemodynamic analysis of radiation-induced damage in common carotid arteries by using color Doppler ultrasonography. *Ultrasonography*, 37(1), pp. 43–49.
- [18] Mohler, E. R., Gornik, H. L., Gerhard-Herman, M., Misra, S., Olin, J. W., & Eugene Zierler, R.(2012). Appropriate use criteria for peripheral vascular ultrasound and physiological testing part I: Arterial ultrasound and physiological testing. *Journal of Vascular Surgery*, 56(1), p.17–51.
- [19] Oqlat, A. A., Matjafri, M. Z., Suardi, N., Oqlat, M. A., Abdelrahman, M. A., & Oqlat, A. A. (2018). A review of medical doppler ultrasonography of blood flow in general and especially in common carotid artery. *Journal of Medical Ultrasound*. 26(1), pp. 3–13.
- [20] Roman, M. J., Naqvi, T. Z., Gardin, J. M., Gerhard-Herman, M., Jaff, M., & Mohler, E. (2006). Clinical application of noninvasive vascular ultrasound in cardiovascular risk stratification: A report from the American Society of Echocardiography and the Society for Vascular Medicine and Biology. *Vascular Medicine*, 11(3), p.201–211.
- [21] Steinman, A. H., Tavakkoli, J., Myers, J. G., Cobbold, R. S. C., & Johnston, K. W. (2001). Sources of error in maximum velocity estimation using linear phased-array Doppler systems with steady flow. *Ultrasound in Medicine and Biology*, 27(5), p.655–664.